Design and experiment of seed furrow cleaning device based on throwing and sliding for no-till maize seeding

Panpan Yuan[1,2], Hongwen Li[1,3*], Caiyun Lu[1,3], Qingjie Wang[1,3], Jin He[1,3], Shenghai Huang[1], Dandan Cui[1]

(1. *College of Engineering, China Agricultural University, Beijing* 100083, *China*;
2. *College of Mechanical and Electrical Engineering, Xinjiang Agricultural University, Urumqi 830052, China*;
3. *Key Laboratory of Agricultural Equipment for Conservation Tillage, Ministry of Agricultural and Rural Affairs, Beijing* 100083, *China*)

Abstract: In order to solve the serious problems of seeds are covered by residual film and overhead by straw during no-till seeding, a seed furrow cleaning device for no-till maize seeding was developed, which adopted a collaborative cleaning method of rotating spring teeth and curved sliding shovel. The movement process and motion trajectory of throwing residual film and straw were constructed. The maximum distance of throwing to one side in horizontal and maximum height in vertical were obtained. The motion trajectory of adjacent spring teeth was analyzed by Matlab, the motion trajectories of adjacent spring teeth at different speeds of 120 r/min, 150 r/min and 180 r/min were achieved, the theoretical analysis results showed that the area of omitted area decreased with the increase of rotation speed. Based on theoretical and simulation analysis of critical parameters, the forward speed of machine, rotation speed of spring teeth, and dip angle between spring teeth and rotary disc were selected as the influencing factor. Straw cleaning rate (SCR) and residual film cleaning rate (RFCR) were selected as the response values for three factors and three levels of orthogonal experiment design. The optimal combination of the selected parameters was obtained, and the field test verification was also conducted. The results showed that the rotation speed of spring teeth, forward speed and dip angle of spring teeth significantly affect SCR and RFCR were in decreasing order. The field test results indicated that when forward speed was 6 km/h, rotation speed of spring teeth was 180 r/min and dip angle of spring teeth was 40°, SCR and RFCR were 88.27% and 84.31%, respectively. This study provides a reference for the development of no-till seeder in Xinjiang and the northwestern regions of China.

Keywords: maize, conservation tillage, no-till seeding, seed furrow cleaning, straw, residual film
DOI: 10.25165/j.ijabe.20221504.7097
Citation: Yuan P P, Li H W, Lu C Y, Wang Q J, He J, Huang S H, et al. Design and experiment of seed furrow cleaning device based on throwing and sliding for no-till maize seeding. Int J Agric & Biol Eng, 2022; 15(4): 95–102.

1 Introduction

The seeding method of covering plastic mulch film has been used for many years in Xinjiang, China, so there are large amounts of residual film in the soil layer[1]. According to statistics, the average amount of residual film in the fields of Xinjiang is more than 260 kg/hm^2[2], which has caused severe white pollution to the agricultural ecological environment[3]. Therefore, it is urgent to explore conservation tillage methods to protect the soil. The no-till seeding is adopted without plastic mulch film. After the previous crops are harvested, the straw and stubble are covered on the farmland and seeding directly without plowing[4,5]. It can reduce wind and water erosion, and improve soil fertility and drought resistance[6-8], which significantly improves the ecological environment in Northwest China.

Currently, the research problems of no-till seeding are concentrated on the straw wind around soil-engaging components during the construction of seed furrows[9-11]. Scholars have carried out extensive research on the "surface" environment[12,13], such as cutting and removing the surface straw to both sides of the proposed seed furrow to ensure the trafficability of no-till seeder[14,15]. For areas with low straw coverage, the self-flowing method of straw is generally adopted to increase the flow space and accelerate the flow of straw by staggered arrangement, increasing ground clearance and adding straw cleaning mechanism[16,17]; Gravity stubble cutting method is used in areas with large straw coverage[18]. The surface straw and stubble are cut by a disc cutter under the gravity of the no-till seeder. The disc cutter process is complicated and requires large positive pressure. Therefore, the mass of no-till seeder is relatively heavy; For two-crop-a-year with large amounts of straw coverage, the power-driven method is adopted[19,20], using high-speed rotary blades to smash, throw, cut, and plow the straw to clear the seedbed without straw coverage by the output power of tractor[21-24]. However, few studies on the "seed furrow" environment, which are the critical point of no-till seeding, the straw and sundries in the seed furrow will directly affect the quality of no-till seeding.

During the field operation of no-till maize seeding in Xinjiang,

Received date: 2021-09-30 **Accepted date:** 2022-03-15
Biographies: Panpan Yuan, PhD candidate, Associate Professor, research interests: conservation tillage and equipment, Email: ypp_xnd@163.com; **Caiyun Lu**, PhD, Associate Professor, research interests: conservation tillage and equipment, Email: lucaiyun@cau.edu.cn; **Qingjie Wang**, PhD, Professor, research interests: conservation tillage and equipment, Email: wangqingjie@cau.edu.cn; **Jin He**, PhD, Professor, research interests: conservation tillage and equipment, Email: hejin@cau.edu.cn; **Shenghai Huang**, PhD candidate, research interests: conservation tillage and equipment, Email: huangshenghaiedu@163.com; **Dandan Cui**, PhD candidate, research interests: conservation tillage and equipment, Email: cuidandan@cau.edu.cn.
***Corresponding author: Hongwen Li**, PhD, Professor, research interests: conservation tillage, agriculture equipment engineering. College of Engineering, China Agriculture University, No.17, Qinghua East Road, Haidian District, Beijing 100083, China. Tel: +86-10-62737300, Email: lhwen@cau.edu.cn.

the author's research team discovered that some seeds would be seeded on the residual film, causing seeds to be covered by the residual film, which will lead to failure of seeds to emerge and affect the emergence rate. The reason for this phenomenon is that the residual film accumulated in the soil layer for many years and are extremely difficult to recover; In addition, in the furrowing process of no-till seeding, some straws cannot be cut off by cutting disc of the no-till seeder and are pressed into seed furrow under the condition of high straw moisture content or large amounts of straw. As a result, the seeds discharged from the seed delivery tube are seeded on straw in the seed furrow, causing the seeds to be overhead by straw[25,26]. Therefore, the working environment in seed furrow is very complicated. The soil is covered with residual film, the residual film contains soil, the residual film and the straw are intertwined. The soil, straw, and residual films form a mixture. It is urgent to explore the cleaning method and device for residual film, straw and other sundries in seed furrow after the furrowing process is completed to provide a clean working environment for no-till seeding.

In this study, a seed furrow cleaning device was proposed for the environmental requirements of no-till seeding in Xinjiang. The motion trajectory and throwing process of straw and residual film were analyzed. The main factors and value ranges that affect the cleaning rate of seed furrow straw and residual film were determined. The orthogonal experimental method was used to explore the optimal parameter combination of the seed furrow cleaning device to solve the problems of seed are covered by residual film and overhead by straw after seed furrow construction. This study provides a reference for the research of no-till seeder in Xinjiang and Northwestern regions.

2 Structure and working principle of seed furrow cleaning device for no-till maize seeding

2.1 Seed furrow cleaning requirements

The planting pattern of no-till maize in Xinjiang is the wide-narrow row with drip irrigation. During no-till seeding, the surface straws are cleaned into wide rows, and the drip irrigation belt is laid in the middle of narrow rows. According to Xinjiang unique soil environment and agronomic requirements, the no-till seeding operations as shown in Figure 1, surface straw cleaning → drip irrigation belt laying → fertilizer furrow opening → fertilizer dropping → seed furrow opening → seed furrow cleaning → seed dropping → soil covering and compaction. Compared with the conventional no-till seeding process, drip irrigation belt laying and seed furrow cleaning are added.

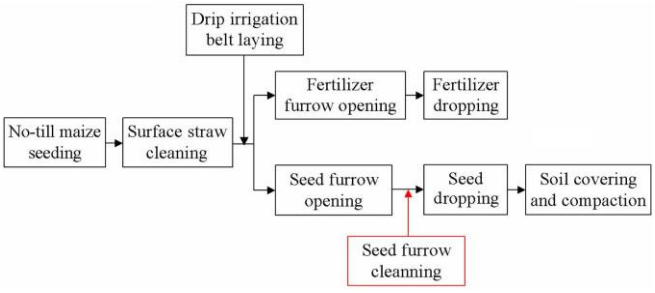

Figure 1 No-till maize seeding operations

As shown in Figure 2, L_1=400 mm, narrow row width; L_2= 600 mm, wide row width; L_3 is the width of the seed furrow, about 40 mm; L_4 is the width of furrow bottom, about 30 mm; H is the height of seed furrow, about 50 mm. After the seed furrow is processed by the furrow opener, the seed furrow cleaning mechanism is operated to throw the residual film and straw out of the seed furrow before the maize seeds fall into the seed furrow.

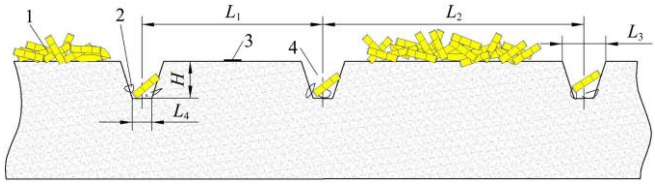

1. Maize straw 2. Residual film 3. Drip irrigation belt 4. Seed furrow

Figure 2 Schematic diagram of operating environment for no-till maize seeding

2.2 Overall structure of seed furrow cleaning device

As shown in Figure 3, a no-till seeder unit with seed furrow cleaning device was designed for use in no-till maize fields. It consisted of surface straw cleaning mechanism, profiling mechanism, furrow opener, seed furrow cleaning device, etc. The seed furrow cleaning device was installed behind the furrow opener of the no-till seeder unit to clean the residual film and straw in the processed seed furrow.

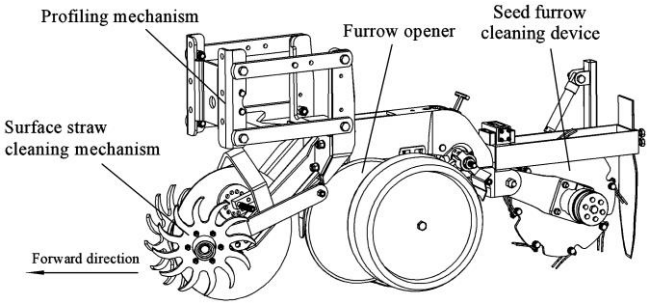

Figure 3 Structural diagram of no-till seeder unit

The specific structure of the seed furrow cleaning device is shown in Figure 4. It mainly consisted of spring teeth, rotary disc, curved sliding shovel, flow speed control valve, frame, and hydraulic system, etc. Among these components, the rotary disc and spring teeth constituted the throwing mechanism. According to different operating conditions, the height of spring teeth can be adjusted by controlling stroke of the hydraulic cylinder. In order to synchronize the curved sliding shovel with spring teeth, the height of curved sliding shovel was adjusted by two positioning bolts. The flow speed control valve was used to control flow of the hydraulic motor to adjust the rotation speed of spring teeth. The spring teeth were installed on the rotary disc at equal intervals. Meanwhile, the working end of the spring teeth has a dip angle with the forward direction. The technical parameters of the seed furrow cleaning device are presented in Table 1.

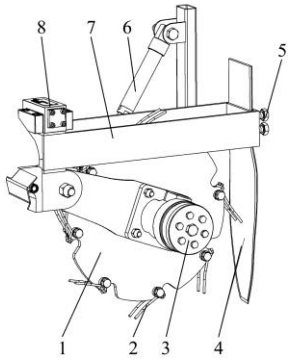

1. Rotary disc 2. Spring teeth 3.Hydraulic motor 4. Curved sliding shovel 5. The adjusting bolt of curved sliding shovel 6. Hydraulic cylinder 7. Frame 8. Flow speed control valve

Figure 4 Structural diagram of seed furrow cleaning device

Table 1 Main parameters of seed furrow cleaning device

Parameters	Value
Driving form	Hydraulic drive
Working speed/km·h^{-1}	4-10
Cleaning width/mm	50
Control range of height adjusting/mm	0-120
Control range of rotational speed/r·min^{-1}	0-300

2.3 Working principle

The seed furrow cleaning device was installed on the no-till seeder and driven by a tractor during operation. The straw and residual films were cleared out of the seed furrow by the combined action of spring teeth and curved sliding shovel. The rotary disc was driven to rotate by a hydraulic motor. Firstly, the curved sliding shovel scooped up the straw and residual film in the seed furrow. Then, the straw and residual film were slid and thrown outside of the seed furrow along the preset direction of the curved sliding shovel by the rotating spring teeth under the action of centrifugal force. Meanwhile, the curved sliding shovel prevented sundries, which were thrown by spring teeth, fall into the seed furrow to avoid secondary pollution to the cleaned seed furrow. The seed delivery tube is arranged behind the curved sliding shovel of the seed furrow cleaning device, and the seeds discharged from the seed metering device fall into the clean seed furrow through the seed delivery tube, then covered with soil for compaction.

3 Design and analysis of key components

3.1 Design of throwing mechanism

The working environment of the throwing mechanism was in seed furrow processed by furrow opener of the no-till seeder, which was directly in contact with the soil, residual film and straw. Therefore, the operating conditions were extremely complicated. As shown in Figure 5, it mainly consisted of spring teeth and rotary disc, etc. The connection between the spring teeth and the rotary disc was fastened in axial and top two directions, which effectively prevented the relative slippage. The fastening hole at the middle of the spring teeth was matched with the threaded hole corresponding to the rotary disc. Moreover, the axial hole of the spring teeth was connected with the rotary disc by bolts. Therefore, the relative position of the top and axial fastening bolt was designed to avoid interference. The edge of the rotary disc had an arc, which was used to match the structure and parameters of the spring teeth.

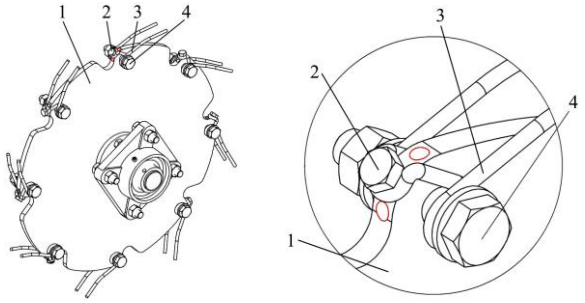

a. Axonometric drawing b. Partial enlarged drawing

1. Rotary disc 2. Top fastening bolt 3. Spring teeth 4. Axial fastening bolt

Figure 5 Schematic diagram of side throwing mechanism

The dip angle between spring teeth and rotary disc would affect the cleaning performance. To obtain a better cleaning effect for seed furrow, three groups of dip angles were set. As shown in Figure 5b, the thread holes marked in the red line were the adjustment holes for spring teeth, 20°, 40°, and 60°, respectively. The installation position of top fastening bolt was adjusted to change the dip angles of spring teeth, while the position of the axial fastening bolt remained unchanged.

The overload elastic protection structure was designed to prevent damage to the spring teeth caused by uneven ground surface and sundries. The spring teeth material was made of carbon spring steel, which has good flexibility and impact resistance. Therefore, the spring teeth had a certain self-adaptive ability when working close to the surface in the seed furrow, which could reduce operation resistance and damage of the spring teeth.

Maize straw can be approximated as a cylinder, so it was easy to slip off due to unbalanced force in the process of picking up with spring teeth; Moreover, the residual film in the seed furrow was mostly fragment, which area was small and difficult to pick up. Therefore, to avoid the straw and residual film slipping from the spring teeth during picking up, the spring teeth with two parallel working teeth were designed, located on both sides of the rotary disc, respectively, as shown in Figure 6. The straw and residual film were picked up by two working teeth and thrown to the rear side. The width of the seed furrow was about 40 mm, so the width between two working teeth was required to be less than 40 mm to maintain the initial structure and avoid damage to the seed furrow. Therefore, the spacing l_1 of the working teeth was 20 mm. Referring to the current residual film collector[27], the diameter d and length l_3 of the spring teeth were 5 mm and 110 mm, respectively. l_4 was the width of the fastening position at the top of spring teeth, which was related to the thickness of rotary disc.

α was the bending angle of spring teeth, and its angle affected the throwing trajectory of straw and residual film. When α=0°, the residual film and straw picked up by spring teeth were thrown back to seed furrow, which could not be thrown out of seed furrow. With the increase of angle α, the width of spring teeth increased. When the width exceeded 40 mm, the seed furrow structure was damaged by spring teeth. It is determined that bending angle α was 25° through many tests.

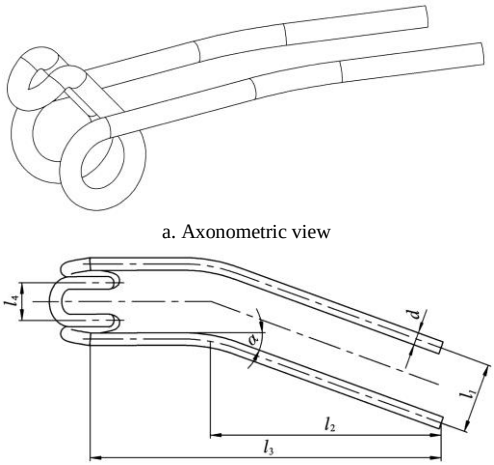

a. Axonometric view

b. Top view

Note: d is the mean diameter of spring teeth, mm; l_1 is the spacing of working spring teeth, mm; l_2 is the projection length of the straight segment of spring teeth, mm; l_3 is the total effective working length of spring teeth, mm; l_4 is the top fastening position width of spring teeth, mm; α is the bending angle, (°).

Figure 6 Structural diagram of spring teeth

3.2 Theoretical and simulation analysis of critical parameters

3.2.1 Movement process and trajectory of spring teeth

As shown in Figure 7, the Cartesian coordinate system was established with the center of the rotating axis as the coordinate origin. The x-axis was the forward direction of the machine, and the z-axis was the vertical direction. The spring teeth touched and moved the straw in seed furrow from point a, and this movement

was "touching straw"; From point *b*, it contacted the surface soil at the bottom of seed furrow, and this movement was "contacting soil"; When the spring teeth moved to point *c*, the tip of spring teeth was left from the soil, and this stage was "leaving soil"; From point *c*, the straw and residual film were carried by spring teeth, and this stage was "carrying"; When the spring teeth moved to point *d*, under the action of gravity and centrifugal force, the straw and residual film were thrown to one side of the seed furrow along the absolute movement direction of spring teeth, and this movement was "throwing". Therefore, the motion trajectory of interaction between spring teeth and straw, residual film, and soil can be divided into five stages: touching straw, contacting soil, leaving soil, carrying and throwing.

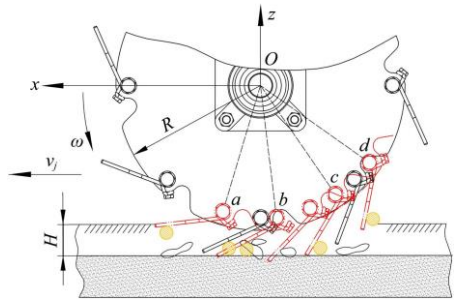

Note: *O* is the gyration center of spring teeth; v_j is the forward speed of the machine, m s^{-1}; ω is the angular velocity of spring teeth movement, rad s^{-1}; *R* is the rotation radius of spring teeth, mm; *H* is the depth of seed furrow, mm; Points *a*, *b*, *c*, and *d* are the critical positions of spring teeth movement to touch straw, contact soil, leave soil and throw away, respectively.

Figure 7 Movement process of spring teeth

The absolute motion of any point on spring teeth was the combination of circular motion of spring teeth rotating around the axis and the linear motion advanced along the machine, which motion trajectory was a regular cycloid. The rotation direction of spring teeth was consistent with the forward direction of the machine. The straw and residual film in the seed furrow were picked up and thrown out of the seed furrow by rotating spring teeth. Motion trajectory of the endpoint on spring teeth is shown in Figure 8.

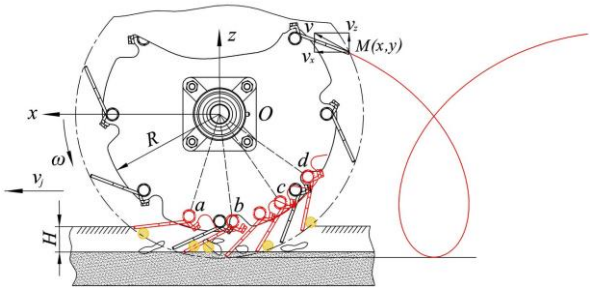

Note: Point *M* is any movement position of the tip of spring teeth; *x* is the displacement in the *x*-axis direction, mm; *z* is the displacement in the *z*-axis direction, mm; *v* is the absolute speed of point *M* on spring teeth, m/s; v_x is the partial velocity of spring teeth in the horizontal direction, m/s; v_z is the partial velocity of spring teeth in the vertical direction, m/s.

Figure 8 Motion trajectory of the endpoint on spring teeth

The movement of any point *M* on spring teeth was analyzed, the coordinates of point *M* was expressed as follows:

$$\begin{cases} x = (R + l_3 \sin\theta)\cos(\omega t) + v_j t \\ z = (R + l_3 \sin\theta)\sin(\omega t) \end{cases} \quad (1)$$

where, *t* is time, s; θ is the dip angle between spring teeth and rotary disc, (°).

The Equation (1) was calculated with derivative of time, the velocity component of spring teeth in *x*-axis and *z*-axis directions were obtained as:

$$\begin{cases} v_x = v_j - (R + l_3 \sin\theta)\omega\sin(\omega t) \\ v_z = (R + l_3 \sin\theta)\cos(\omega t) \end{cases} \quad (2)$$

Therefore, the absolute velocity equation of any point *M* on the spring teeth was:

$$v = \sqrt{v_j^2 + (R + l_3 \sin\theta)^2\omega^2 - 2v_j(R + l_3 \sin\theta)\omega\sin\omega t} \quad (3)$$

3.2.2 Determination of spring teeth speed

The rotation speed of spring teeth had a significant influence on the cleaning effect of seed furrow. The rotation speed of spring teeth was too low to throw out the straw and residual film. However, if the rotation speed of spring teeth was too high, the seed furrow structure would be damaged. In order to throw out the straw and residual film while avoiding the influence of high-speed rotation of spring teeth on seed furrow structure, the rotation speed of spring teeth needs to determine.

To achieve effective throwing, the conditions of throwing straw and residual film to the rear side should be satisfied during the rotation movement of spring teeth, which had a resultant backward velocity. Specifically, the ratio of the linear velocity *v* of the spring teeth circular motion to the forward speed v_j of the machine was λ>1, as shown in Equation (4):

$$v > v_j \quad (4)$$

$$\omega(R + l_3\sin\theta) > v_j \quad (5)$$

According to the forward speed of no-till maize seeder during operation, valued v_j=2.22 m/s, then

$$\omega(R + l_3\sin\theta) > 2.22 \quad (6)$$

Therefore

$$n > \frac{2.22 \times 60}{2\pi(R + l_3 \sin\theta)} \quad (7)$$

where, *n* is the rotation speed of spring teeth, r/min.

The gyration radius *R*=150 mm, length of spring teeth l_3= 110 mm, and dip angle θ=20°, 40°, and 60° respectively, which were substituted into Equation (7). Therefore, the rotation speed of spring teeth *n*>113 r/min was determined to meet the operation requirements of rotation speed at different dip angles.

3.2.3 Kinematics analysis of throwing straw and residual film

In order to study the motion trajectory and law of straw and residual film were thrown by spring teeth, the instantaneous motion of straw and residual film thrown was analyzed. The straw and residual film are simplified as a particle, and the spring teeth rotated uniformly. Meantime, the influence of air resistance and the collision between straw and residual film were ignored. The process of straw and residual film throwing is shown in Figure 9.

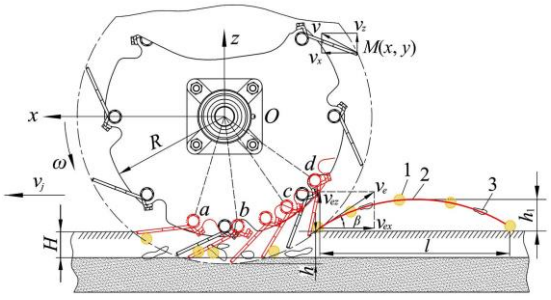

1. Maize straw 2. Throwing trajectory 3. Residual film

Figure 9 Kinematics analysis of maize straw and residual film throwing process

Point *e* was the critical point where the straw and residual film separated from the spring teeth, then the straw and residual film were thrown to the rear side of seed furrow along the absolute movement direction of spring teeth. The instantaneous velocity at which the straw and residual films were thrown point *e* is expressed

as below:

$$v_e=\omega(R+l_3\sin\theta) \tag{8}$$

where, v_e is the instantaneous velocity of straw and residual film at point *e*, m/s.

The velocity components of spring teeth in the *x*-axis and the *z*-axis directions are v_{ex} and v_{ez}, respectively, which are calculated by Equation (9)

$$\begin{cases} v_{ex}=v_e\cos\beta=\omega(R+l_3\sin\theta-h) \\ v_{ez}=v_e\sin\beta=\omega\sqrt{2(R+l_3\sin\theta)h-h^2} \end{cases} \tag{9}$$

where, β is the included angle between the instantaneous direction of throwing and horizontal direction, (°); h is the vertical distance between the starting position of throwing and the bottom of seed furrow, mm.

The straw and residual film were separated from spring teeth and thrown out to move in a parabolic. The motion trajectory equations are shown below

$$\begin{cases} x_e=-\sqrt{2(R+l_3\sin\theta)h-h^2}-(R+l_3\sin\theta-h)\omega t \\ y_e=(R+l_3\sin\theta)\omega t \\ z_e=h-R-l_3\sin\theta+\sqrt{2(R+l_3\sin\theta)h-h^2}\omega t-\dfrac{gt^2}{2} \end{cases} \tag{10}$$

where, x_e is the distance that straw and residual film are thrown in the *x*-axis direction, mm; y_e is the distance that straw and residual film are thrown in the *y*-axis direction, mm; z_e is the distance that straw and residual film are thrown in the *z*-axis direction, mm.

According to Equations (9) and (10), the maximum distance l that the straw and residual film were thrown to backward horizontally by spring teeth was obtained as follow

$$\begin{aligned} l&=\frac{2v_e^2\sin\beta\cos\beta}{g}\cos\alpha \\ &=\frac{2\omega^2(R+l_3\sin\theta-h)\sqrt{2(R+l_3\sin\theta)h-h^2}}{g}\cos\alpha \end{aligned} \tag{11}$$

where, g is the acceleration of gravity, m/s^2.

The maximum distance L that the straw and residual film were thrown to the side in the horizontal plane perpendicular to the forward direction of the machine was calculated.

$$L=l\tan\alpha=\frac{2\omega^2(R+l_3\sin\theta-h)\sqrt{2(R+l_3\sin\theta)h-h^2}}{g}\sin a \tag{12}$$

Similarly, the maximum height h_1 that the straw and residual films are thrown to the vertical direction was calculated.

$$h_1=\frac{(v_e\sin\beta)^2}{2g}=\frac{\omega^2[(R+l_3\sin\theta)h-h^2]}{2g} \tag{13}$$

The straw and residual films are thrown from point *e*. With the rotation of the spring teeth, the throwing velocity v_e at different positions was the same. However, the direction was different. When the velocity of spring teeth v_{ex}=0, the straw and residual film was no longer thrown to the outside of seed furrow. It could be obtained from Equations (11), Equations (12) and Equations (13) that the throwing distance of straw and residual film in backward horizontally, rear side and vertical directions changes with the change of v_e direction. When the included angle between v_e and *x*-axis direction β=45°, the maximum throwing distance was obtained. It could be seen from the above equations that the main factors affecting throwing distance were: angular velocity of spring teeth ω, dip angle θ, working length l_3 and bending angle α of spring teeth. When rotation speed n was 120 to 180 r/min, dip angle θ was 20° to 60°, and the bending angle α was 25°, rotary disc R was 150 mm, length of spring teeth l_3 was 110 mm, and substituting into Equations (12) and (13). Then, the maximum distance that the straw and residual film was thrown to one side in horizontal was 239.3 to 747.0 mm, and the maximum height that the straw and residual film was thrown to vertical direction was 141.7 to 442.2 mm.

3.2.4 Simulation analysis of spring teeth motion trajectory

With the forward movement of the no-till seeder, the circular motion of adjacent spring teeth formed staggered cycloids, so there may be omitted areas between adjacent spring teeth. The omitted areas were mainly determined by the forward speed, the rotation speed of spring teeth and the number of spring teeth distributed in the circumferential direction.

In order to explore the relationship between omitted areas and the above parameters, Matlab software was used to obtain the motion trajectory of two adjacent spring teeth. Under different parameter combinations, the motion trajectory of spring teeth would change, and the area of the omitted area would also change, but the periodic change trend of motion trajectory was the same. According to the result of design and theoretical analysis, the simulation parameters were selected as machine forward speed v_j = 2.22 m/s, radius of rotary disc R=150 mm, rotation speed of spring teeth n=120 r/min, 150 r/min and 180 r/min, respectively, running time t=1 s, number of spring teeth distributed in the circumferential direction n=8. Then, the above parameters were substituted into Equation (1), the absolute motion trajectory of spring teeth. The position, where the endpoint of spring teeth is at the highest point, was the initial position of motion simulation. The motion trajectories of adjacent spring teeth and the omitted areas are shown in Figure 10.

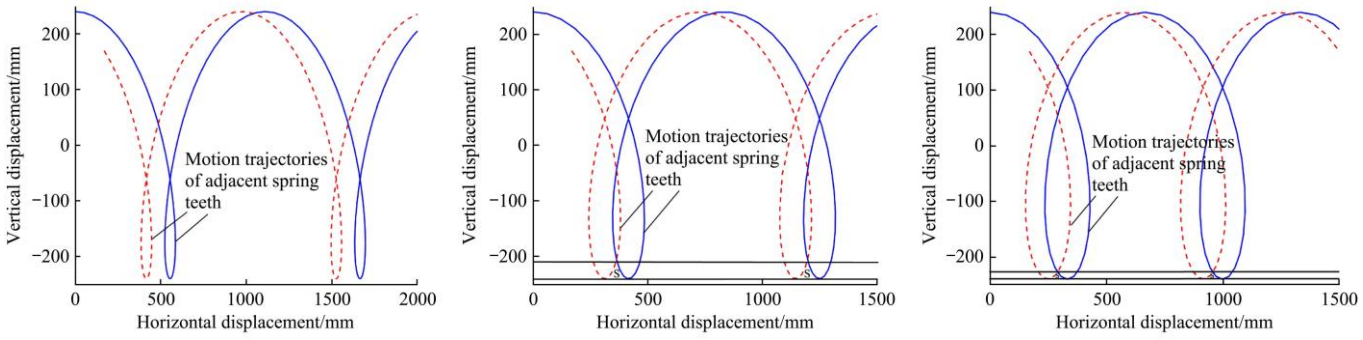

a. 120 r/min b. 150 r/min c. 180 r/min

Figure 10 Motion trajectories of adjacent spring teeth

It could be seen from Figure 10a that when the rotation speed of spring teeth was 120 r/min, there was no intersection point between the motion trajectories of the adjacent spring teeth. To be specific, when the rotation speed of spring teeth was 120 r/min, it just met the speed requirements obtained by Equation (7), so there was an omitted area between motion trajectories of adjacent

spring teeth, and the area of the omitted area was larger.

When the rotation speed of spring teeth was 150 r/min and 180 r/min, the motion trajectories of adjacent spring teeth are shown in Figures 10b and 10c, respectively. The motion trajectories of adjacent spring teeth were intersecting, and the distance between intersection point and lowest point of the motion trajectory decreased with the increasing of rotation speed, that is, the area of omitted area decreased with the increasing of rotation speed. Therefore, the rotation speed of spring teeth was one of the significant parameters affecting seed furrow cleaning performance.

4 Materials and methods

4.1 Experimental materials

The field experiment was conducted on April 28 and 29, 2021 at Bole Experimental Station (81°43′43″E, 44°56′34″N) of China Institute for Conservation Tillage of China Agricultural University, Xinjiang, China. The soil moisture content was 14.35%, and the average soil compaction at depth of 50 mm was 1120.8 kPa. The previous crop of the experimental field was maize after harvest in the autumn of 2020, which straw mulching quantity and average moisture content were 1.64 kg/m^2 and 11.73 %, respectively. The content of the residual film in soil layer was 0.017 kg/m^2.

The experimental instruments were as follows: LX904 tractor; DT-2235B digital tachometer, which measurement accuracy is 0.05%; SC-900 soil compaction experimenter, which range and accuracy are 7000 kPa and 1 kPa, respectively; Electronic balance, which range is 0-1000 g; Soil moisture experimenter, tape measure, vernier caliper, etc. The seed furrow cleaning experimental device is shown in Figure 11.

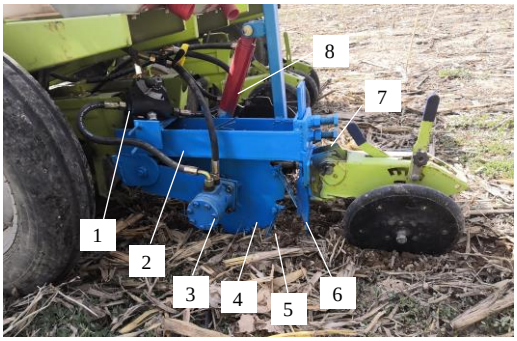

1. Flow speed control valve 2. Frame 3. Hydraulic motor 4. Rotary disc 5. Spring teeth 6. Curved sliding shovel 7. Adjusting bolt of curved sliding shovel 8. Hydraulic cylinder

Figure 11 Field experiment of seed furrow cleaning device for no-till seeding

4.2 Experimental methods

There were many factors that impacted the performance of the seed furrow cleaning device, such as forward speed, diameter of rotary disc, rotation speed of spring teeth, bending angle of spring teeth, and dip angle between spring teeth and rotary disc, etc. According to kinematic analysis of the side throwing mechanism, the forward speed, rotation speed of spring teeth, and dip angle between spring teeth and rotary disc were determined to be the main factors affecting the cleaning effect. Therefore, the forward speed, rotation speed of spring teeth and dip angle between spring teeth and rotary disc were selected as the experimental factors.

Table 2 Experimental factors and levels

Level	Machine forward speed v_j/km h^{-1}	Rotation speed of spring teeth r_s/r min^{-1}	Dip angle of spring teeth a_s/(°)
1	6	120	20
2	8	150	40
3	10	180	60

The $L_9(3^4)$ orthogonal experimental method was used to obtain the optimal parameters combination. The setting of level values of the factors is listed in Table 2.

4.3 Experiment evaluation indicators

To evaluate the performance of the seed furrow cleaning device, straw cleaning rate (SCR) and residual film cleaning rate (RFCR) were selected as evaluation indicators. According to GB/T 20865-2017 "no or little tillage fertilizer-seeder"[28] in China, the operation performance of seed furrow cleaning device for no-till maize seeding was inspected.

The mass of straws and weeds in the width of sowing stripper unit length was measured before operation. The residual mass of straws and weeds in the width of sowing strip was measured by an electronic balance after the operation. Therefore, SCR was calculated by Equation (14)

$$\varphi = \frac{m_1 - m_2}{m_1} \times 100\% \quad (14)$$

where, φ is the straw cleaning rate, %; m_1 is the mass of straws and weeds before operation, kg; m_2 is the residual mass of straws and weeds after operation, kg.

The residual film on the surface in operation area were picked up manually before operation. When the seed furrow cleaning operation was completed, the mass of residual film from the seed furrow cleaned to the surface, and the mass of the residual film that had not been cleaned in the seed furrow were measured, respectively. Therefore, RFCR was calculated by Equation (15)

$$\eta = \frac{m_3}{m_3 + m_4} \times 100\% \quad (15)$$

Where, η is the residual film cleaning rate, %; m_3 is the mass of residual film from the seed furrow cleaned to the surface, kg; m_4 is the mass of residual film that had not been cleaned, kg.

5 Results and discussion

5.1 Effects of operation parameters on SCR and RFCR

The influences of forward speed, rotation speed of spring teeth and dip angle of spring teeth on the SCR and RFCR are listed in Table 3.

Table 3 Orthogonal experiment results of seed furrow cleaning

No.	Machine forward speed v_j	Rotation speed of spring teeth r_s	Dip angle of spring teeth a_s	Straw cleaning rate φ	Residual film cleaning rate η
1	1	1	1	73.42	72.51
2	1	2	2	85.10	86.84
3	1	3	3	92.13	83.92
4	2	1	2	74.91	70.56
5	2	2	3	82.57	77.34
6	2	3	1	89.82	78.59
7	3	1	3	71.28	70.42
8	3	2	1	80.96	82.05
9	3	3	2	90.14	85.32
$K_{\varphi1}$	83.55	73.20	81.40		
$K_{\varphi2}$	82.43	82.88	83.38		
$K_{\varphi3}$	80.79	90.70	81.99		
$K_{\eta1}$	81.09	71.16	77.72		
$K_{\eta2}$	75.50	82.08	80.91		
$K_{\eta3}$	79.26	82.61	77.23		
R_φ	2.76	17.49	1.98		
R_η	5.59	11.45	3.68		

The range R_φ and R_η were analyzed and results showed that the rotation speed of spring teeth, forward speed and dip angle of spring teeth significantly affect SCR and RFCR were in decreasing order. The optimal parameter combination was: $v_{j1}r_{s3}a_{s2}$. To be specific, forward speed was 6 km/h, rotation speed of spring teeth was 180 r/min and dip angle of spring teeth was 40 °. Meanwhile, overall observation found that SCR was higher than RFCR under the same structure and parameters.

To further test the significance of difference in the mean value of samples, analysis of variance (ANOVA) was utilized (at 95% confidence interval) to evaluate the effects. The results are listed in Table 4. Forward speed was significantly related to SCR, and extremely significantly related to RFCR. The rotation speed of spring teeth was extremely significantly related to SCR and RFCR. The dip angle of spring teeth had no significant effect on SCR, but which had a very significant effect on RFCR.

Table 4 ANOVA analysis on SCR and RFCR

Source of variation	Straw cleaning rate /%					Residual film cleaning rate /%				
	Sum of squares	DF	Mean square	*F* value	*p* value	Sum of squares	DF	Mean square	*F* value	*p* value
v_j	11.54	2	5.77	15.40	0.061	48.81	2	24.41	158.34	0.006
r_s	460.74	2	230.37	615.07	0.002	250.41	2	125.21	812.32	0.001
a_s	6.22	2	3.11	8.30	0.108	23.96	2	11.98	77.72	0.013
Error	0.75	2	0.38			0.31	2	0.15		
Total	479.25	8				323.49	8			

Note: $p<0.01$ means extremely significant, $0.01<p<0.05$ means very significant, $0.05<p<0.1$ means significant. DF: Degree of freedom.

To verify the accuracy of the optimal operation parameters, the operation parameters of validation experiment were set as: forward speed was 6 km/h, rotation speed of spring teeth was 180 r/min and dip angle of spring teeth was 40 °. The validation experiment was conducted on the same field conditions as previous experiments. Three repetitions were performed and the average value was calculated. The effect after field experiment is shown in Figure 12. Under the optimal operation parameters, SCR and RFCR were 88.27% and 84.31%, respectively, cleaning performance got a significant improvement for no-till seeder.

a. Seed furrow after cleaning b. Seed furrow after covering soil

Figure 12 Effect after field experiment

In the operation parameters of validation experiment, 6 points were randomly selected to measure the throwing distance of straw and residual film. The results are listed in Table 5.

Table 5 Throwing distance of maize straw and residual film

No.	The throwing distance of maize straw/mm	The throwing distance of residual film/mm
1	304.3	113.7
2	272.1	158.2
3	231.3	106.8
4	314.6	127.3
5	252.7	105.1
6	265.2	94.4
Mean value	273.4	117.6

It can be realized that the maximum and mean value throwing distance of maize straw were 314.6 mm and 273.4 mm, respectively, and the maximum and mean value throwing distance of residual film were 158.2 mm and 117.6 mm, respectively. The maize straw and residual film were thrown into the wide row (600 mm) by seed furrow cleaning device, so it will not affect the operation of other adjacent rows.

5.2 Discussion

According to the result of ANOVA analysis, the rotation speed of spring teeth had an extremely significant effect on SCR and RFCR. When the rotation speed of spring teeth was 120 r/min, SCR and RFCR were all relatively low. The experimental results were consistent with theoretical and simulation results. When the rotation speed of spring teeth is higher than 180 r/min, the high-speed rotation of spring teeth may disturb the processed seed furrow with the increase of rotation speed, which may affect the initial structure of seed furrow, moreover, increase the energy consumption. Therefore, the rotation speed of spring teeth should not be too high.

The dip angles of spring teeth were set at 20 °, 40 °, and 60 °, respectively, however, the diameter of maize straw is generally 18 to 30 mm, and the volume is relatively large. So, when the dip angle of spring teeth was adjusted by 20 °, it had little effect on SCR. The dip angle of spring teeth had no significant effect on SCR.

The residual film is accumulated in the soil layer for many years, its mechanical properties are poor, and the residual film is easy to break during cleaning; Meanwhile, the residual film has a small area, which is easy to slip off and difficult to pick up. Therefore, RFCR was lower than SCR under the same structure and parameters.

The throwing distance of residual film is smaller than maize straw, the main reason is that the residual film has the characteristics of extremely light, adsorption and flexibility.

6 Conclusions

In this study, a seed furrow cleaning device for no-till seeding was developed for environmental requirements in Xinjiang, China. The operation parameters of seed furrow cleaning were obtained using orthogonal method. The performance of the seed furrow cleaning device was evaluated in field conditions. The main conclusions were drawn as below.

To solve the problems of seed are covered by residual film and overhead by straw, a seed furrow cleaning device for no-till maize seeding was designed, which was installed behind the furrow opener of no-till seeder to clean the residual film and straw in the processed seed furrow. The straw and residual film were slid and thrown to outside of the seed furrow by collaborative cleaning method of rotating spring teeth and curved sliding shovel.

The trajectory of spring teeth and motion model of throwing

residual film and straw were constructed. The results indicated that the maximum distance of throwing to one side in horizontal was 239.3 to 747.0 mm, and the maximum height in vertical was 141.7 to 442.2 mm. The motion trajectory of two adjacent spring teeth and change of omitted area were analyzed by Matlab, and the results showed that the area of omitted area decreased with the increasing of rotation speed.

The orthogonal experiment results showed that rotation speed of spring teeth, forward speed and dip angle of spring teeth significantly affect SCR and RFCR were in decreasing order. The field test results indicated that when forward speed was 6 km/h, rotation speed of spring teeth was 180 r/min and dip angle of spring teeth was 40°, SCR and RFCR were 88.27% and 84.31%, respectively. The maximum throwing distances of maize straw and residual film were 314.6 mm and 158.2 mm, respectively.

Acknowledgements

This work was supported by the National Natural Science Foundation of China (Grant No. 52165039), Xinjiang Agricultural Machinery R&D, Manufacturing, Promotion, and Application Integration Project (Grant No. YTHSD2022-14), China Agriculture Research System of MOF and MARA (Grant No. CARS-03), Xinjiang Key Laboratory of Intelligent Agricultural Equipment. Gratitude should be expressed to all the members of Conservation Tillage Research Centre.

[References]

[1] Hu C, Wang X F, Wang S G, Lu B, Guo W S, Liu C J, et al. Impact of agricultural residual plastic film on the growth and yield of drip-irrigated cotton in arid region of Xinjiang, China. Int J Agric & Biol Eng, 2020; 13(1): 160–169.

[2] Liang R Q, Chen X G, Zhang B C, Meng H W, Jiang P, Peng X B, et al. Problems and countermeasures of recycling methods and resource reuse of residual film in cotton fields of Xinjiang. Transactions of the CSAE, 2019; 35(16): 1–13. (in Chinese)

[3] Guo W S, Hu C, He X W, Wang L, Hou S L, Wang X F. Construction of virtual mulch film model based on discrete element method and simulation of its physical mechanical properties. Int J Agric & Biol Eng, 2020; 13(4): 211–218.

[4] Pittelkow C M, Liang X Q, Linquist B A, Groenigen K J, Lee J, Lundy M E, et al. Productivity limits and potentials of the principles of conservation agriculture. Nature, 2015; 517: 365–368.

[5] Sidhu H S, Singh M, Singh Y, Blackwell J, Lohan S K, Humphreys E, et al. Development and evaluation of the turbo happy seeder for sowing wheat into heavy rice residues in NW India. Field Crops Research, 2015; 184: 201–212.

[6] Ye R Z, Parajuli B, Ducey T F, Novak J M, Bauer P J, Szogi A A. Cover cropping increased phosphorus stocks in surface sandy Ultisols under long-term conservation and conventional tillage. Agronomy Journal, 2020; 112(4): 3163–3173.

[7] Piazza G, Pellegrino E, Moscatelli M C, Ercoli L. Long-term conservation tillage and nitrogen fertilization effects on soil aggregate distribution, nutrient stocks and enzymatic activities in bulk soil and occluded microaggregates. Soil and Tillage Research, 2020; 196: 104482. doi: 10.1016/j.still.2019.104482.

[8] Rolf D, Theodor F, Amir K, Li H. Current status of adoption of no-till farming in the world and some of its main benefits. Int J Agric & Biol Eng, 2010; 3(1): 1–25.

[9] Hou S Y, Chen H T, Zou Z, Wei Z P, Zhang Y L. Design and test of lateral stubble cleaning blade for corn stubble field. Transactions of the CSAE, 2020; 36(2): 59－69. (in Chinese)

[10] Fallahi S, Raoufat M H. Row-crop planter attachments in a conservation tillage system: a comparative study. Soil and Tillage Research, 2008; 98(1): 27–34.

[11] Huang Y X, Gao P Y, Zhang Q K, Shen H, Zhu R X, Shi J T. Design and experiment of grass soil separation device with combination of stubble cutting and grass guiding used for no-till Planter. Transactions of the CSAM, 2020; 51(5): 67–78. (in Chinese)

[12] Ahmad F, Qiu B J, Ding Q S, Ding W M, Khan Z M, Shoaib M, et al. Discrete element method simulation of disc type furrow openers in paddy soil. Int J Agric & Biol Eng, 2020; 13(4): 103–110.

[13] Sharipov G M, Paraforos D S, Pulatov A S, Griepentrog H W. Dynamic performance of a no-till seeding assembly. Biosystems Engineering, 2017; 158: 75–94.

[14] Sharma V K. Development and performance evaluation of a multi-toolbar no-till seed drill for surface managed loose straw conditions after combining. Pantnagar: G. B. Pant University of Agriculture and Technology, 2014.

[15] Lin J, Li B F, Li H Z. Design and experiment of archimedes spiral type stubble breaking ditching device and stubble breaking anti blocking device. Transactions of the CSAE, 2015; 31(17): 10–19. (in Chinese)

[16] Yuan P P, Li H W, Jiang G J, He J, Lu C Y, Huang S H. Design and experiment of straw cleaning device for wide-narrow maize no-tillage sowing strip in drip irrigation area. Transactions of the CSAM, 2021; 52(6):43–52. (in Chinese)

[17] He J, Li H W, Chen H T, Lu C Y, Wang Q J. Research progress of conservation tillage technology and machine. Transactions of the CSAM, 2018; 49(4): 1–19. (in Chinese)

[18] Ahmad F, Ding W M, Ding Q S, Hussain M, Jabran K. Forces and straw cutting performance of double disc furrow opener in no-till paddy soil. Plos One, 2015; 10(3): e0119648. doi: 10.1371/journal.pone.0119648.

[19] Niu M M, Fang H M, Chandio F A, Shi C, Xue Y F, Liu H. Design and experiment of separating-guiding anti-blocking mechanism for no-tillage maize planter. Transactions of the CSAM, 2019; 50(8): 52–58. (in Chinese)

[20] Chen H T, Hou L, Hou S Y, Li Y, Min S Y, Chai Y D. Design and optimization experiment of anti-blocking mechanism of no-tillage planter for grand ridge with raw corn stubble. Transactions of the CSAM, 2018; 49(8): 59–67. (in Chinese)

[21] Matin M A, Fielke J M, Desbiolles J M A. Torque and energy characteristics for strip-tillage cultivation when cutting furrows using three designs of rotary blade. Biosystems Engineering, 2015; 129: 329–340.

[22] Cao X P, Wang Q J, Li H W, He J, Lu C Y, Yu C C. Design and experiment of active rotating collective straw-cleaner. Transactions of the CSAE, 2021; 37(6): 26–34. (in Chinese)

[23] Zhao S H, Liu H P, Hou L T, Zhang X, Yuan Y W, Yang Y Q. Development of deep fertilizing no-tillage segmented maize sowing opener using discrete element method. Transactions of the CSAE, 2021; 37(13): 1–10. (in Chinese)

[24] Godsey C, Kochenower R, Taylor R. Strip-till considerations in Oklahoma. Oklahoma Cooperative Extension Service, 2015; PSS–2134.

[25] Liu Z J, Liu L J, Yang X J, Zhao Z B, Liu X Q. Design and experiment of no-till precision planter for corn. Transactions of the CSAE, 2016; 32(Supp.2): 1–6. (in Chinese)

[26] Luo W W, Hu Z C, Wu F, Gu F W, Xu H B, Chen Y Q. Design and optimization for smashed straw guide device of wheat clean area planter under full straw field. Transactions of the CSAE, 2019; 35(18): 1–10. (in Chinese)

[27] Xie J H, Tang W, Cao S L, Han Y J, Zhang Y, Yang Y X, et al. Design and experiment of tooth chain compound residual film recovery machine. Transactions of the CSAE, 2020; 36(1): 11–19. (in Chinese)

[28] GB/T 20865-2017. No or little-tillage fertilizes-seeder. Beijing: Standards Press of China, 2017. (in Chinese)